The Janus kinase inhibitor JTE-052 improves skin barrier function through suppressing signal transducer and activator of transcription 3 signaling

Wataru Amano, DVM,[a,b] Saeko Nakajima, MD, PhD,[a] Hayato Kunugi, PhD,[b] Yasuharu Numata, MS,[b] Akihiko Kitoh, MD, PhD,[a] Gyohei Egawa, MD, PhD,[a] Teruki Dainichi, MD, PhD,[a] Tetsuya Honda, MD, PhD,[a] Atsushi Otsuka, MD, PhD,[a] Yukari Kimoto, MS,[b] Yasuo Yamamoto, MS,[b] Atsuo Tanimoto, MS,[b] Mutsuyoshi Matsushita, PhD,[b] Yoshiki Miyachi, MD, PhD,[a] and Kenji Kabashima, MD, PhD[a,c] *Kyoto, Tokyo, and Saitama, Japan*

Background: Barrier disruption and the resulting continuous exposure to allergens are presumed to be responsible for the development of atopic dermatitis (AD). However, the mechanism through which skin barrier function is disrupted in patients with AD remains unclear.
Objectives: Taking into account the fact that the T_H2 milieu impairs keratinocyte terminal differentiation, we sought to clarify our hypothesis that the Janus kinase (JAK)–signal transducer and activator of transcription (STAT) pathway plays a critical role in skin barrier function and can be a therapeutic target for AD.
Methods: We analyzed the mechanism of keratinocyte differentiation using a microarray and small interfering RNA targeting STATs. We studied the effect of the JAK inhibitor JTE-052 on keratinocyte differentiation using the human skin equivalent model and normal human epidermal keratinocytes. We applied topical JAK inhibitor onto NC/Nga mice, dry skin model mice, and human skin grafted to immunocompromised mice.
Results: IL-4 and IL-13 downregulated genes involved in keratinocyte differentiation. STAT3 and STAT6 are involved in keratinocyte differentiation and chemokine production by keratinocytes, respectively. Topical application of the JAK inhibitor suppressed STAT3 activation and improved skin barrier function, permitting increases in levels of terminal differentiation proteins, such as filaggrin, and natural moisturizing factors in models of AD and dry skin and in human skin.
Conclusion: STAT3 signaling is a key element that regulates keratinocyte differentiation. The JAK inhibitor can be a new therapeutic tool for the treatment of disrupted barrier function in patients with AD. (J Allergy Clin Immunol 2015;136:667-77.)

Key words: *Atopic dermatitis, filaggrin, signal transducer and activator of transcription 3, Janus kinase inhibitor, keratinocyte differentiation*

The key function of the epidermis is to serve as a physiologic barrier between the organism and its environment. The outermost cornified layer (stratum corneum [SC]) serves as a physical barrier, minimizing water loss from the body and protecting against environmental insults, including irritants and allergens.[1,2] Barrier disruption and the resulting continuous exposure to allergens are presumed to be responsible for the development of atopic dermatitis (AD).[3-5] Skin barrier function depends on the normal differentiation of keratinocytes, as experiments with genetically modified mice, such as filaggrin (FLG)–deficient mice, have shown.[6-8] Keratinocyte differentiation is characterized by a protein expression pattern that varies depending on its localization.[9] It has been demonstrated with gene-targeted mice that normal keratinocyte differentiation is indispensable for skin barrier function.[6,8,10]

FLG is one of the molecules expressed during terminal keratinocyte differentiation. FLG is produced in the granular layer (stratum granulosum [SG]) as profilaggrin, a precursor protein consisting of 10 to 12 tandem repeats of monomeric FLG peptide. During the SG to SC transition, profilaggrin is cleaved into multiple FLG monomers that provide physical strength by aggregating the keratin bundles.[11] At the outer layers of the SC, FLG is degraded into free amino acids, collectively known as natural moisturizing factors (NMFs), which contribute to epidermal hydration and barrier function.[12]

From [a]the Department of Dermatology, Kyoto University Graduate School of Medicine; [b]the Central Pharmaceutical Research Institute, Japan Tobacco, Tokyo; and [c]PRESTO, Japan Science and Technology Agency, Saitama.

Supported in part by Grants-in-Aid for Scientific Research from the Ministry of Education, Culture, Sports, Science, and Technology (to K.K.) and from the Ministry of Health, Labour and Welfare (to K.K.); Precursory Research for Embryonic Science and Technology (to K.K.); a Grant-in-Aid from the Japan Society for the Promotion of Science Fellows (to S.N.), and by Japan Tobacco.

Disclosure of potential conflict of interest: W. Amano is employed by and owns stock in Japan Tobacco; Japan Tobacco and Kyoto University co-own a pending patent application regarding methods for skin barrier function-related skin diseases. S. Nakajima has received research support from the Japan Society for the Promotion of Science. H. Kunugi, Y. Numata, Y. Yamamoto, and M. Matsushita are employed by Japan Tobacco. Y. Kimoto and A. Tanimoto are employed by Japan Tobacco; Japan Tobacco and Kyoto University co-own a pending patent application regarding methods for skin barrier function-related skin diseases. K. Kabashima has received research support from the Ministry of Education, Culture, Sports, Science, and Technology; the Ministry of Health, Labour and Welfare; Precursory Research for Embryonic Science and Technology; and a joint research grant by Japan Tobacco; Japan Tobacco and Kyoto University co-own a pending patent application regarding methods for skin barrier function-related skin diseases. The rest of the authors declare that they have no relevant conflicts of interest.

Received for publication November 6, 2014; revised March 18, 2015; accepted for publication March 27, 2015.

Available online June 24, 2015.

Corresponding author: Kenji Kabashima, MD, PhD, Department of Dermatology, Kyoto University Graduate School of Medicine, 54 Shogoin Kawaharamachi, Sakyo-ku, Kyoto 606-8507, Japan. E-mail: kaba@kuhp.kyoto-u.ac.jp. OR: Mutsuyoshi Matsushita, PhD, Central Pharmaceutical Research Institute, Japan Tobacco, 1-1 Murasaki-cho Takatsuki, Osaka 569-1125, Japan. E-mail: mutsuyoshi.matsushita@jt.com.

0091-6749/$36.00

http://dx.doi.org/10.1016/j.jaci.2015.03.051

Abbreviations used
AD: Atopic dermatitis
AEW: Acetone/ether/water
DMSO: Dimethyl sulfoxide
FLG: Filaggrin
GO: Gene Ontology
H&E: Hematoxylin and eosin
JAK: Janus kinase
LOR: Loricrin
NHEK: Normal human epidermal keratinocyte
NMF: Natural moisturizing factors
SC: Stratum corneum
SG: Stratum granulosum
siRNA: Small interfering RNA
SPF: Specific pathogen-free
STAT: Signal transducer and activator of transcription
TEWL: Transepidermal water loss

Loss-of-function mutations in the *FLG* gene are one of the genetic risk factors responsible for AD[4,13] and multiple other allergic diseases, including asthma.[14-16] Importantly, it has been reported that FLG and NMF production are downregulated in patients with AD, regardless of their *FLG* genotype.[5,17] Expression levels of *FLG* and loricrin *(LOR)* mRNA in keratinocytes were significantly downregulated in the presence of IL-4 and IL-13 (IL-4/IL-13) *in vitro*,[17,18] suggesting that the T_H2 cytokine milieu contributes to the impairment of epidermal differentiation.[19-21] A variety of cytokines, including IL-4/IL-13, exert their biological effects by binding to their cognate receptors, some of which activate Janus kinases (JAKs), a small family of cytoplasmic protein tyrosine kinases comprising JAK1, JAK2, JAK3, and tyrosine kinase 2.[22] JAKs then activate signal transducer and activator of transcription (STAT) proteins to induce expression of specific genes.[23] Several investigations have indicated that the activation of JAK-STAT signaling occurs in the skin of patients with AD,[24] but the roles of JAK-STAT signaling in skin barrier function remain largely unclear.

In the present study we examined the role of JAK-STAT signaling in skin barrier function. Microarray and Gene Ontology (GO) analysis of the reconstructed human skin equivalent model revealed that IL-4/IL-13 downregulated genes involved in keratinocyte differentiation, most of which were counteracted by JTE-052, a novel JAK inhibitor. Using normal human epidermal keratinocytes (NHEKs), we found that IL-4/IL-13 phosphorylates STAT3, which inhibited keratinocyte differentiation. Topical administration of the JAK inhibitor improved skin barrier function, permitting increases in FLG and NMF levels in a murine model of AD and dry skin. Moreover, the JAK inhibitor promoted the production of FLG and NMFs in human skin that had been grafted onto immunocompromised mice. These findings demonstrate the feasibility of JAK inhibitors as possible new therapeutic agents for AD that work by improving skin barrier function.

METHODS

Animals

C57BL/6J (B6) and BALB/c nu/nu (nude) mice were purchased from SLC (Shizuoka, Japan) and maintained on a 12-hour light/dark cycle at a temperature of 24°C and humidity of 50% ± 10% under specific pathogen-free (SPF) conditions at Kyoto University Graduate School of Medicine. NC/Nga mice were purchased from SLC and maintained under either SPF or conventional conditions with fur mite infection. All experimental procedures were approved by the Institutional Animal Care and Use Committee of Kyoto University Graduate School of Medicine.

Drugs and reagents

The JAK inhibitor JTE-052 was synthesized at Japan Tobacco (Osaka, Japan). In an enzymatic assay JTE-052 inhibited JAK1, JAK2, JAK3, and tyrosine kinase 2, with inhibitory concentrations of 50% of 2.8, 2.6, 13, and 58 nmol/L, respectively.[25] For *in vitro* studies, JTE-052 was dissolved in dimethyl sulfoxide (DMSO) and added to reach a final DMSO concentration of less than 0.1%. For *in vivo* studies, JTE-052 was diluted in acetone containing 1% (vol/vol) of DMSO and topically applied daily.

Cell culture and transfection

NHEKs (Kurabo Industries, Osaka, Japan) were cultured as described previously.[26] Keratinocyte differentiation was induced by culturing the NHEKs in a culture medium containing 1.5 mmol/L Ca^{2+} for 5 days. Cells were transfected with either small interfering RNA (siRNA) for STATs or control siRNA (Cell Signaling Technology, Beverly, Mass) by using HiPerFect Reagent (Qiagen, Valencia, Calif). Culture medium was changed to a medium containing 1.5 mmol/L Ca^{2+} at 24 hours after transfection, and cells were cultured for 72 hours in the presence or absence of IL-4 (100 ng/mL) and IL-13 (100 ng/mL). The total concentration of siRNA was 50 nmol/L. As a reconstructed human skin equivalent model, TESTSKIN (Toyobo, Osaka, Japan) was cultured in the presence or absence of 1000 nmol/L JTE-052 and 20 ng/mL recombinant human IL-4 and IL-13 (R&D Systems, Minneapolis, Minn).

Murine dry skin model

B6 mice were treated with acetone/ether/water (AEW), as described previously, to induce dry skin.[27] Briefly, the interior surface of each mouse ear was soaked with a mixture of acetone and diethyl ether (1:1) for 30 seconds and then with water for 30 seconds twice daily for the indicated periods.

Human skin graft model

After informed consent was obtained, human skin samples were obtained from unused portions of grafts, most of which had been intended for use in surgery and were transplanted onto immunodeficient athymic nude mice. The protocol was approved by the Ethical Committee for the Study of Human Analysis at Kyoto University Medical School and the Ethics Committee of the Central Pharmaceutical Research Institute of Japan Tobacco, which stipulate adherence to the rules laid out in the Declaration of Helsinki.

Statistical analysis

Unless otherwise indicated, data are presented as means ± SDs, and each result represents one of the 3 independent experiments. Differences between 2 groups were analyzed by means of 1-way ANOVA, and P values were calculated by using to the 2-tailed t test. For multiple comparisons, statistical significance was assessed with the Dunnett test (for homoscedastic data) or Steel test (for heteroscedastic data) after homoscedasticity analysis with the Bartlett test. For the meta-analysis of microarray data, NextBio software (www.nextbio.com) was used to assess P values.[28] P values of less than .05 are considered significant and indicated by an asterisk in the figures.

RESULTS

IL-4/IL-13 inhibited keratinocyte differentiation, possibly through JAK-STAT signaling

It has previously been reported that mRNA expression levels of T_H2 cytokines, including IL-4 and IL-13, are increased in the skin lesions of patients with AD[17,29] and that IL-4 and IL-13 modulate the expression levels of genes relevant to keratinocyte

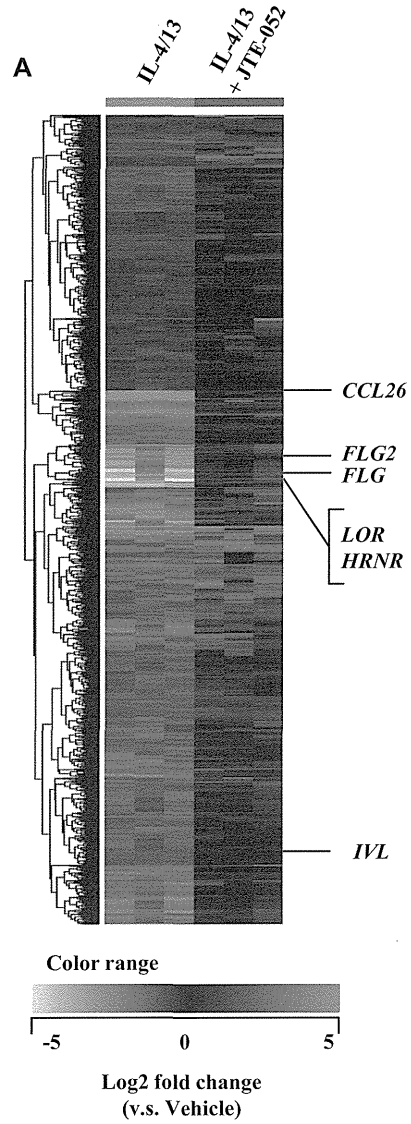

B

Rank	GO	Common genes	Direction	*P*-value
1	Keratinization	18	down	2.00E-27
2	Keratinocyte differentiation	21	down	3.90E-26
3	Epidermal cell differentiation	23	down	4.00E-25
4	Epidermis development	39	down	1.60E-20
5	Epithelial cell differentiation	31	down	1.20E-19
6	Proteinaceous extracellular matrix	37	down	1.30E-18
7	Extracellular matrix	40	down	1.50E-18
8	Inflammatory response	29	up	4.40E-16
9	Cytokine activity	18	up	6.20E-16
10	Response to metal ion	25	down	2.10E-13

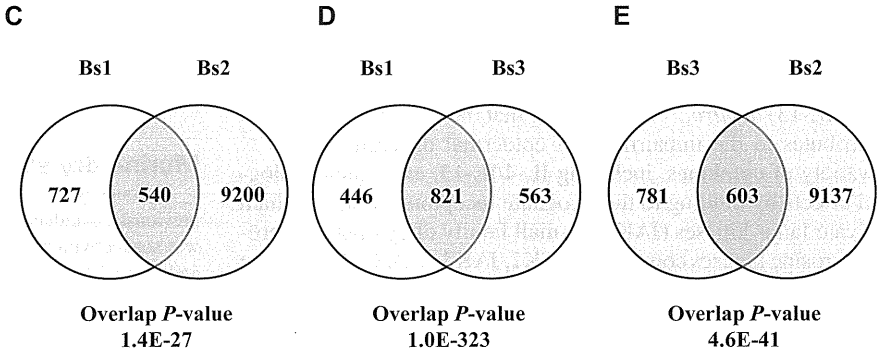

FIG 1. IL-4/IL-13 dominantly downregulated gene groups involved in keratinocyte differentiation. **A,** Heat map of genes in TESTSKIN treated with IL-4/IL-13 in the absence *(left)* or presence *(right)* of JTE-052 (n = 3). **B,** Enriched GO terms for genes with altered expression induced by IL-4/IL-13. **C-E,** Correlation analyses between the genes differentially expressed in (C) IL-4/IL-13–treated samples (Bioset; Bs1) and genes with altered expression in AD skin (GSE16161; Bs2; Fig 1, *C*), Bs1 and IL-4/IL-13 plus JTE-052-treated samples (Bs3; Fig 1, *D*), and Bs3 and Bs2 (Fig 1, *E*).

differentiation, such as *FLG*.[18] However, it remains largely unclear how IL-4 and IL-13 affect keratinocyte differentiation.

First, we performed microarray analysis to determine the effect of IL-4/IL-13 on keratinocytes. We prepared TESTSKIN as a human skin equivalent reconstructed model. Expression levels of 1267 genes in the epidermal layer of TESTSKIN were changed at least 2-fold by treatment with IL-4/IL-13 from their expressions in untreated TESTSKIN (Fig 1, *A*, left panel). GO analysis was performed by using GO terms associated with biological processes to clarify the biological effect of IL-4/IL-13 on keratinocytes (for the definition of GO terms, please refer http://geneontology.org/).[30] GO analysis revealed that IL-4/IL-13 predominantly downregulated the gene groups related to certain functions, such as keratinization, keratinocyte differentiation, and epidermal cell differentiation (Fig 1, *B*), which suggests that keratinocyte differentiation is inhibited under T_H2 conditions, such as AD. Then we performed correlation analysis between gene expression changes induced by IL-4/IL-13 in TESTSKIN (Bs1) and gene changes in the skin of patients with AD (accession no. GSE16161[31]; Bs2). These analyses demonstrated that 540 genes overlapped significantly ($P = 1.4 \times 10^{-27}$) and that these genes were positively correlated: 163 were upregulated, and 220 were downregulated ($P = 3.6 \times 10^{-19}$ and $P = 1.6 \times 10^{-37}$, respectively; Fig 1, *C*, and see Fig E1, *A*, in this article's Online Repository at www.jacionline.org).

It has been reported that cytokines, including IL-4/IL-13, exert their function through JAK-STAT activation.[23] To explore the implications of this, we next investigated the effect of a JAK inhibitor on TESTSKIN in the presence of IL-4/IL-13 *in vitro*.

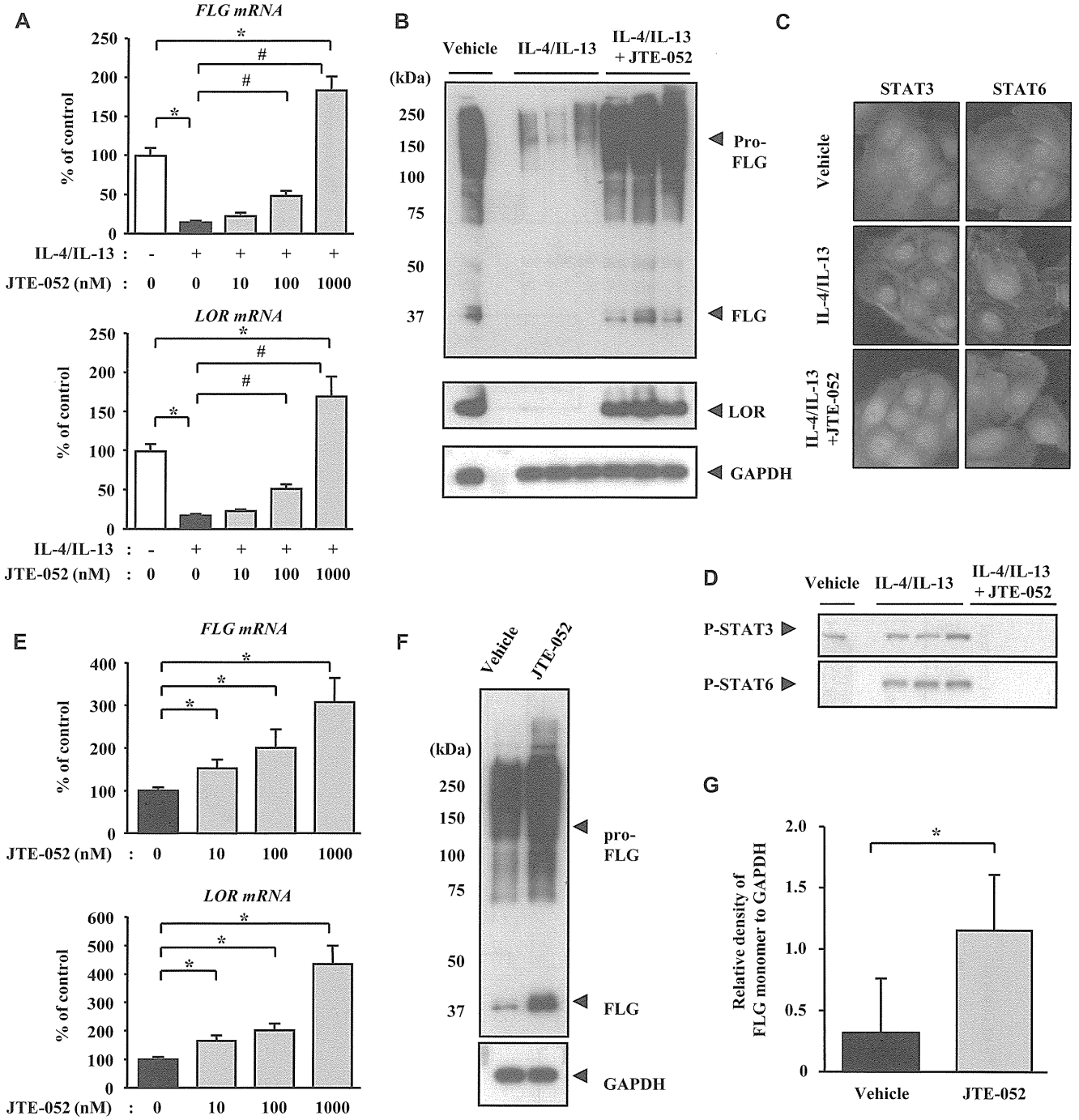

FIG 2. The JAK inhibitor promoted keratinocyte differentiation. Vehicle or the JAK inhibitor JTE-052 was applied to the culture medium for 5 days in the presence **(A-D)** or absence **(E-G)** of IL-4/IL-13. Fig 2, *A*, Effects of JTE-052 on *FLG* and *LOR* mRNA expression of NHEKs in the presence of IL-4/IL-13. Effects of the compound were calculated and represented as percentage change from mean control value. Fig 2, *B*, FLG and LOR protein production in TESTSKIN. Fig 2, *C*, Immunofluorescent staining of STAT3 and STAT6 *(green)* or β-actin *(red)* in NHEKs. Fig 2, *D*, Phosphorylation of STAT3 and STAT6 in TESTSKIN. Fig 2, *E*, Effects of JTE-052 on *FLG* and *LOR* mRNA expression in NHEKs. Fig 2, *F*, FLG protein production in TESTSKIN. Fig 2, *G*, Relative density of the FLG monomer to glyceraldehyde-3-phosphate dehydrogenase *(GAPDH)* in TESTSKIN (n = 6). Fig 2, *A* and *E*, Data represent the average of 3 independent experiments ± SEMs. *$P < .05$ versus vehicle (*t* test). #$P < .05$ versus IL-4/IL-13 treatment (Steel test).

A number of genes induced by IL-4/IL-13 treatment were suppressed by 1000 nmol/L of the JAK inhibitor JTE-052 (Fig 1, *A*, right panel). Expression levels of 1384 genes were changed by JAK inhibitor treatment at least 2-fold from their expression levels in IL-4/IL-13–treated TESTSKIN; these genes (Bs3) were negatively correlated with the genes exhibiting altered

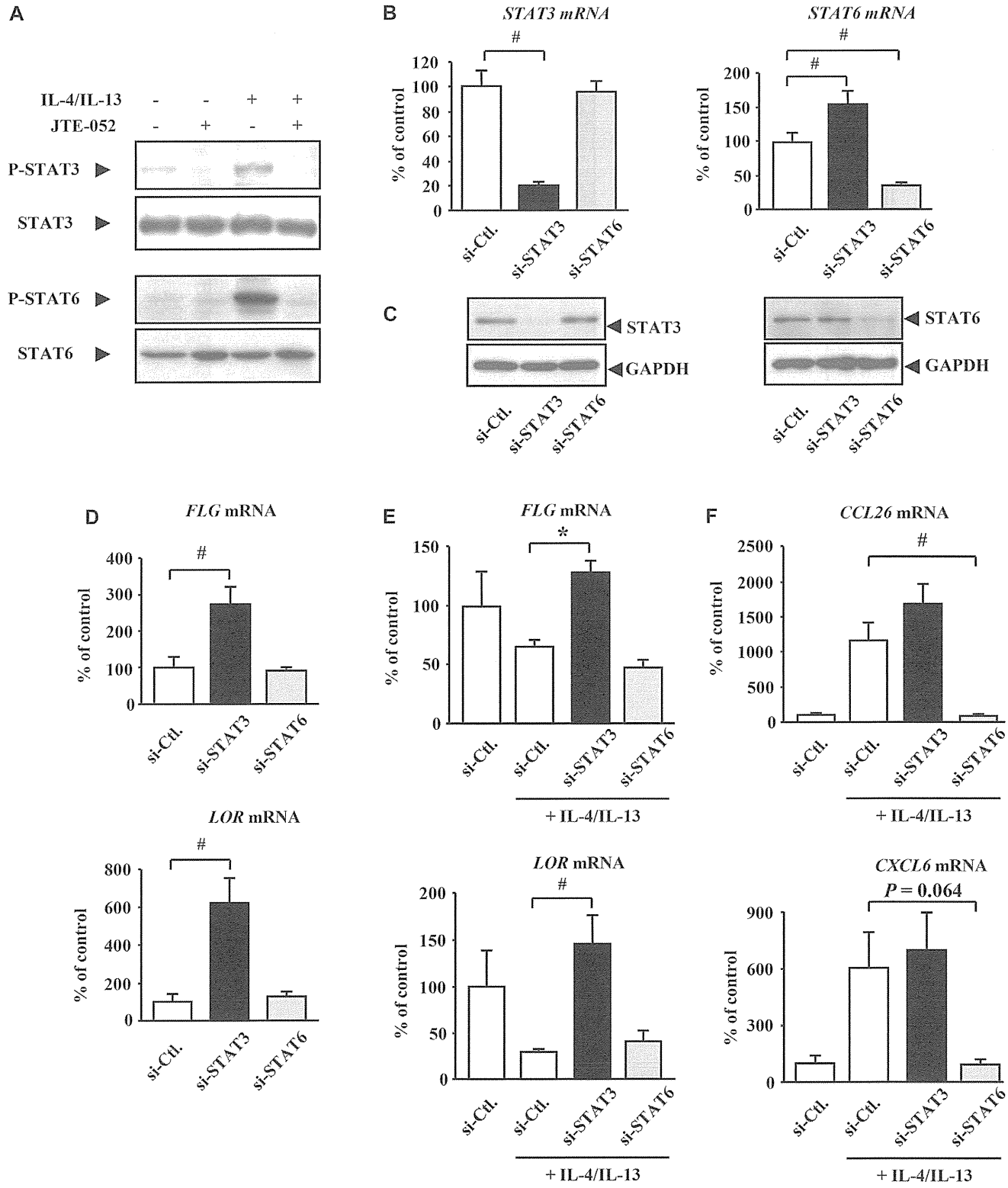

FIG 3. STAT3, but not STAT6, is a predominant negatively acting transcriptional factor for keratinocyte differentiation. **A,** Phosphorylation of STAT3 and STAT6 in NHEKs. **B** and **C**, Silencing effects of siRNAs on *STAT* mRNA (n = 7 of each group; Fig 3, *B*) and protein (Fig 3, *C*) expression. **D** and **E**, *FLG* and *LOR* mRNA expression in the absence (Fig 3, *D*) or presence (Fig 3, *E*) of IL-4/IL-13. **F,** *CCL26* and *CXCL6* mRNA expression in the presence of IL-4/IL-13 (n = 7 of each group). Data are presented as means ± SEMs. **P* < .05 versus control siRNA (Dunnett test). #*P* < .05 versus control siRNA (Steel test).

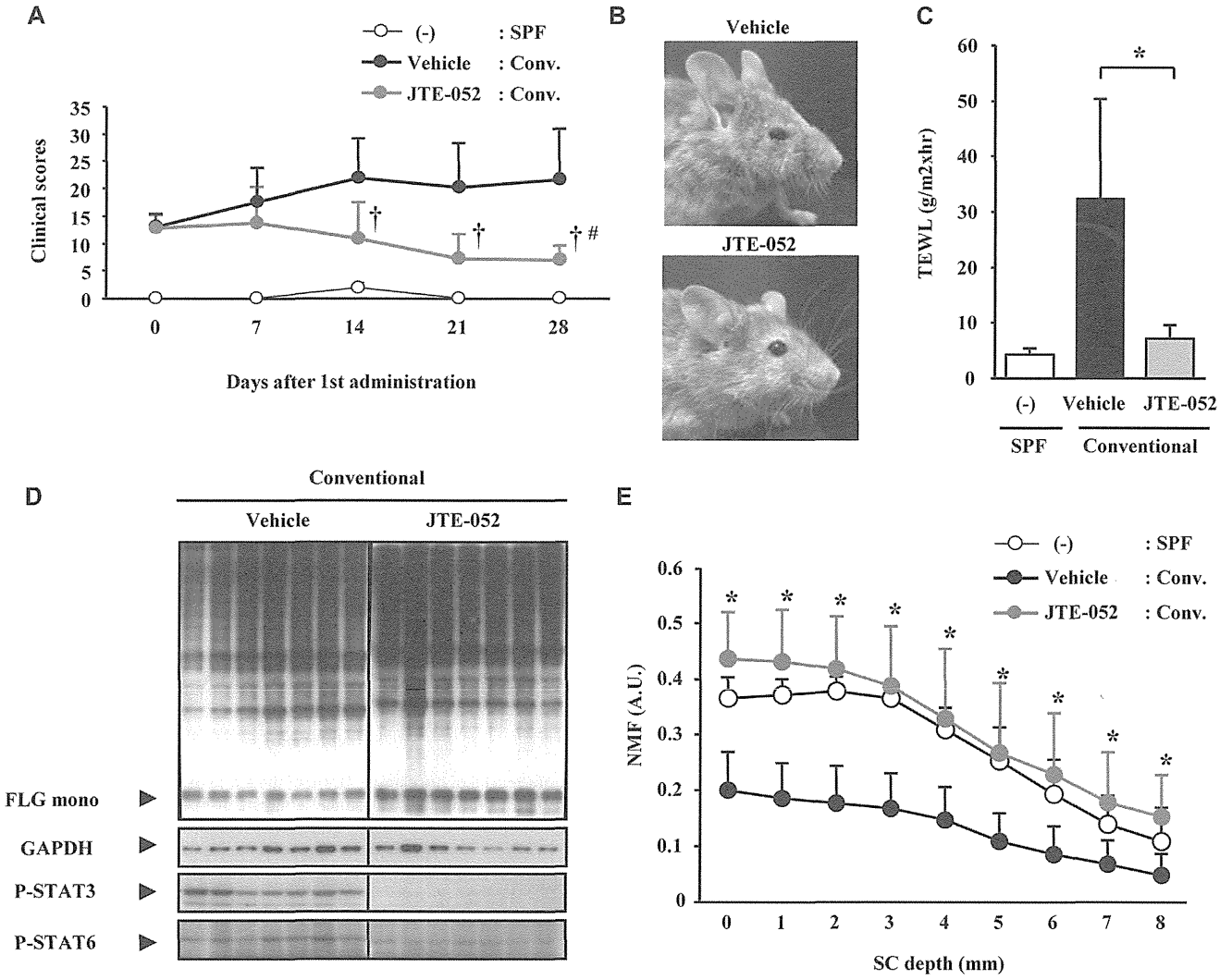

FIG 4. Topical administration of the JAK inhibitor ameliorated barrier disruption in NC/Nga mice (n = 7 or 8). **A,** Time course of total clinical severity scores. **B,** Clinical photographs of NC/Nga mice on day 28. **C,** TEWL of the ear of NC/Nga mice on day 28. **D,** FLG protein and phosphorylated STATs in the epidermis of NC/Nga mouse ear on day 28. **E,** NMF concentration in the epidermis of NC/Nga mice ear on day 28. *$P < .05$ versus vehicle-treated mice (t test). †$P < .05$ versus vehicle-treated mice (Wilcoxon rank sum test). #$P < .05$ versus JTE-052–treated mice at day 0 (Steel test).

expression levels in IL-4/IL-13–treated TESTSKIN (Bs1; 821 overlapped, $P = 1.0 \times 10^{-323}$; Fig 1, *D*, and see Fig E1, *B*) and AD-affected skin (Bs2; 603 overlapped, $P = 4.6 \times 10^{-41}$; Fig 1, *E*, and see Fig E1, *C*). These data suggest that IL-4/IL-13 treatment imitates the conditions of human AD skin lesions in the epidermis and that IL-4/IL-13 downregulates epidermal differentiation through JAK-STAT signaling. Therefore inhibition of JAK activities in epidermal cells might be a possible means of improving disrupted keratinocyte differentiation by reversing the changes in gene expression seen in AD lesions.

JAK inhibitor promoted differentiation of keratinocytes, regardless of the presence or absence of IL-4/IL-13

Next, we sought to directly evaluate the effects of the JAK inhibitor on keratinocyte differentiation. Consistent with our microarray analysis using a human skin equivalent model and AD skin lesions and previous reports,[17,18] IL-4/IL-13 directly downregulated expression levels of *FLG* and *LOR* mRNA after a 5-day NHEK incubation (Fig 2, *A*). In addition, the JAK inhibitor restored *FLG* and *LOR* mRNA expression levels in the presence of IL-4/IL-13 in a dose-dependent manner. Because FLG and LOR are produced in the SG layer of the epidermis, the above findings suggest that the JAK inhibitor might enhance keratinocyte terminal differentiation. During epidermal terminal differentiation, profilaggrin (approximately 400 kDa) is cleaved to monomeric FLG (37 kDa), which plays an important role in barrier formation in mammalian skin.[32] We used the epidermal layer of TESTSKIN to evaluate profilaggrin, FLG monomer, and LOR production as a keratinocyte terminal differentiation molecule. IL-4/IL-13 decreased production levels of these proteins, and JAK inhibitor treatment restored them (Fig 2, *B*).

It has been reported that IL-4 and IL-13 activate both STAT3 and STAT6 signaling in lymphocytes, such as B cells,[33,34] but the responsible STAT signaling through IL-4/IL-13 in keratinocyte

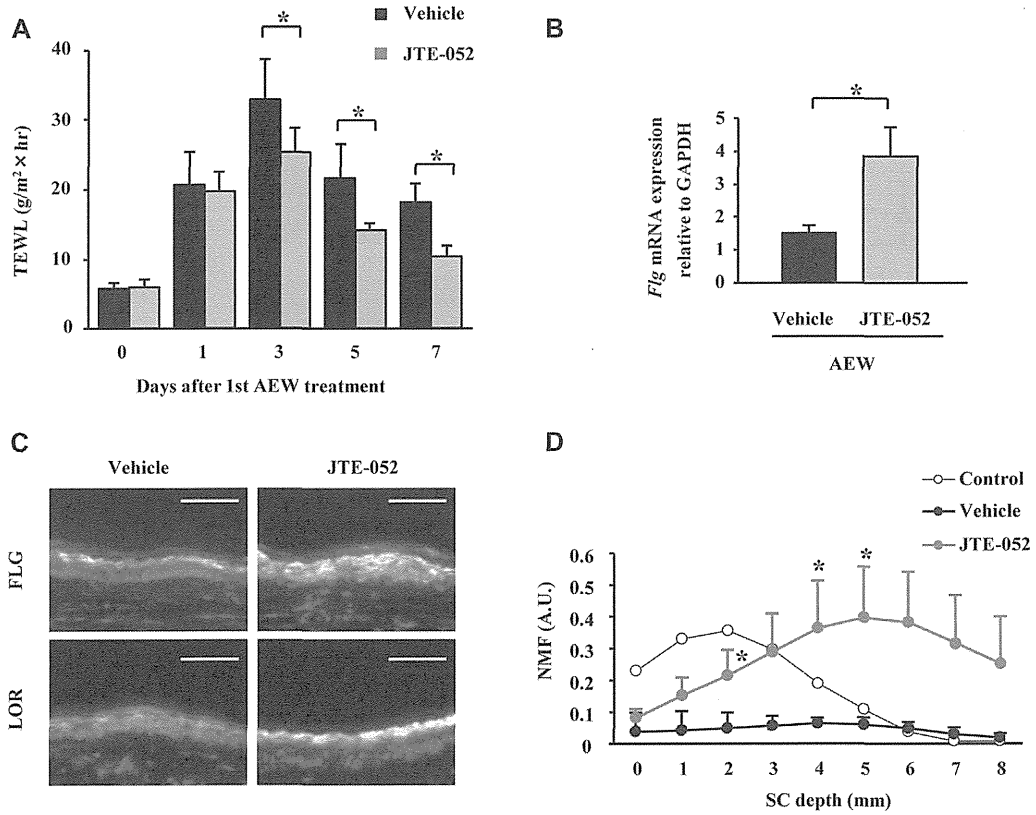

FIG 5. The JAK inhibitor ameliorated barrier function in a mouse model of dry skin. **A,** TEWL of the ear of dry skin model mice. **B,** *Flg* mRNA expression in the ear on day 3. **C,** Immunohistochemical analysis of FLG protein *(green)* in the ear on day 7. Nuclei were counterstained with DAPI *(blue). Scale bar* = 50 μm. **D,** NMF concentration in the epidermis of the ear on day 7 (n = 4). **P* < .05 versus vehicle-treated mice (*t* test).

differentiation is unclear. To clarify this issue, we first evaluated STAT localization in NHEKs after IL-4/IL-13 stimulation. We found that both STAT3 and STAT6 were translocated into the nucleus after IL-4/IL-13 stimulation and that this translocation was suppressed by the JAK inhibitor. These findings indicate that IL-4/IL-13 regulates transcriptional activation of both STAT3 and STAT6 in keratinocytes (Fig 2, *C*). In keeping with this finding, immunoblot analysis revealed that both STAT3 and STAT6 were phosphorylated in the presence of IL-4/IL-13 and that both were inhibited by the JAK inhibitor (Fig 2, *D*). Of note, no remarkable phosphorylation of STAT1, STAT2, and STAT5 was detected based on the presence of IL-4/IL-13 (see Fig E2 in this article's Online Repository at www.jacionline.org). We also found that STAT3 was phosphorylated even in the absence of IL-4/IL-13, suggesting that STAT3 is constitutively activated in the cultured keratinocytes, whereas phosphorylation of STAT6 was not. Intriguingly, we observed that the extent of restoration by the JAK inhibitor in the presence of IL-4/IL-13 was significantly greater than that seen in the absence of IL-4/IL-13 (Fig 2, *A*). This finding suggests that JAK-STAT signaling was activated endogenously, even without addition of IL-4/IL-13. In accordance with our hypothesis, the JAK inhibitor increased both *FLG* and *LOR* mRNA expression levels, even in the absence of IL-4/IL-13, 5 days after incubation of NHEKs (Fig 2, *E*). Moreover, phosphorylated STAT3 was more strongly detected 5 days after incubation than 1 day after incubation (see Fig E3, *A*, in this article's Online Repository at www.jacionline.org). Consistently, the JAK inhibitor increased monomeric FLG (Fig 2, *F* and *G*) and LOR (see Fig E3, *B*) protein production and inhibited STAT3 phosphorylation (see Fig E3, *C*) in TESTSKIN compared with vehicle. These findings suggest that phosphorylated STATs might play an important role in keratinocyte differentiation, irrespective of the presence of IL-4/IL-13.

STAT3, but not STAT6, was a responsible factor involved in modulating keratinocyte differentiation

We then sought to investigate the effects of STAT3 and STAT6 in keratinocyte differentiation. Both STAT3 and STAT6 were phosphorylated by IL-4/IL-13, which was abrogated by JTE-052 (Fig 3, *A*). We examined the effect of each STAT's silencing on the mRNA expression levels of FLG and LOR. We found that small interfering RNA (siRNA) targeting STAT3 and STAT6 reduced mRNA and protein expression levels, respectively (Fig 3, *B* and *C*). siRNA analysis revealed that *FLG* and *LOR* mRNA expression levels were upregulated by siRNA of STAT3 but not by siRNA of STAT6 (Fig 3, *D*). Consistently, interference with STAT6 had no effect on *FLG* and *LOR* mRNA expression levels in the presence of IL-4/IL-13, whereas interference with STAT3 upregulated *FLG* and *LOR* mRNA expression (Fig 3, *E*). These data suggest that STAT3, but not STAT6, is a key transcription factor involved in modulating the differentiation of keratinocytes and that the JAK

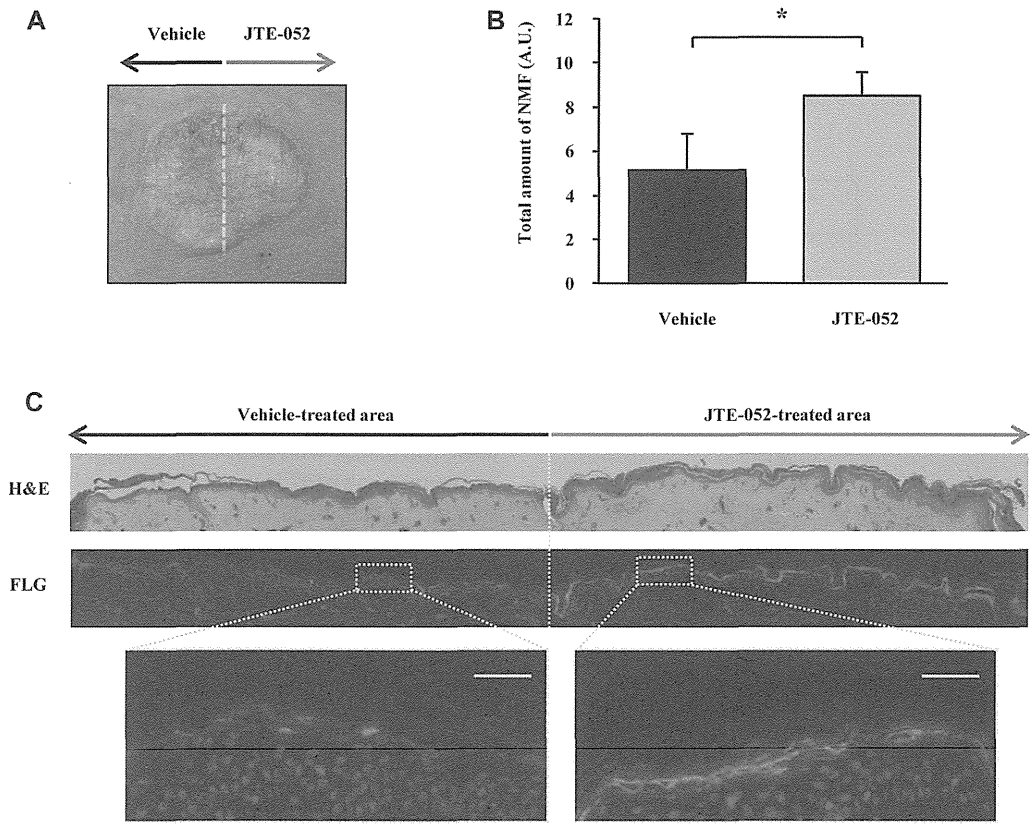

FIG 6. The JAK inhibitor enhanced NMF and FLG protein expression in human skin. **A,** Representative image of grated human skin on athymic nude mice. **B,** Total amount of NMF in the vehicle- or 0.5% JTE-052–treated area (integral value of SC depth from 0-28 μm). **C,** H&E staining *(upper panel)* and immunostaining of FLG *(lower panel, red)* of histologic sections from grafted human skin. *Scale bar* = 50 μm. **P* < .05 versus vehicle treatment (*t* test).

inhibitor can enhance keratinocyte differentiation by inhibiting STAT3 signaling.

There were 1267 genes with mRNA levels that were significantly changed in the epidermal layer of TESTSKIN by addition of IL-4/IL-13, as revealed through microarray analysis (Fig 1, *C*). Among the 100 most dramatically upregulated genes, we found that the mRNA level of the T_H2 chemokine *CCL26*, which might be involved in the pathogenesis of AD,[35,36] was significantly upregulated by the addition of IL-4/IL-13 (see Table E1 in this article's Online Repository at www.jacionline.org, rank 2). It has been reported that the production of CCL26 is induced by T_H2 cytokines in cells of the keratinocyte cell line HaCaT.[36] Consistent with the previous report, IL-4/IL-13 increased *CCL26* mRNA expression levels, which were decreased by interference with STAT6 but not STAT3 (Fig 3, *F*). Similarly, other chemokine *(CXCL6)* mRNA expression upregulated by IL-4/IL-13 in TESTSKIN (see Table E1, rank 15) was suppressed by interference with STAT6 but not STAT3 (Fig 3, *F*). Therefore STAT3 and STAT6 have different effects on keratinocytes under the T_H2 milieu, attenuating keratinocyte differentiation and promoting chemokine production, respectively.

Topical application of the JAK inhibitor ameliorated spontaneous AD-like skin inflammation and barrier disruption in NC/Nga mice

NC/Nga mice have spontaneous AD-like dermatitis about 8 weeks after birth when they are raised under conventional conditions (conventional mice) but not when they are raised under SPF conditions (SPF mice).[37] We used 8- to 9-week-old NC/Nga mice with mild to severe skin inflammation as an animal model of AD to evaluate the therapeutic effect of the JAK inhibitor *in vivo*. JTE-052 (0.5% [wt/vol] in acetone, 40 μL/d) or vehicle (acetone containing 1% [vol/vol] of DMSO) was topically applied once daily onto the skin of conventional mice. In vehicle-treated NC/Nga conventional mice clinical manifestations gradually became worse, but clinical manifestations in NC/Nga conventional mice treated with topical application of the JAK inhibitor were significantly milder than those in vehicle-treated mice (Fig 4, *A* and *B*). In addition, the JAK inhibitor significantly decreased clinical scores: clinical scores measured 3 to 4 weeks after treatment were significantly lower than those measured on day 0 (Fig 4, *A*). These findings suggest that topical application of the JAK inhibitor not only prevents exacerbation of AD-like skin inflammation but also improves its clinical manifestations.

In addition, oral or topical application of the JAK inhibitor suppressed ear-swelling responses in an antigen-induced chronic allergic dermatitis model using NC/Nga mice (see Fig E4 in this article's Online Repository at www.jacionline.org). Of note, the efficacy of the JAK inhibitor was observed dose dependently (see Fig E4, *A*) and was comparable or even better when compared with that of orally administrated cyclosporine (see Fig E4, *A*) or topically applied tacrolimus ointment (see Fig E4, *B*).

Transepidermal water loss (TEWL) is used as a measurement of skin barrier function.[38] On day 28, TEWL of the ear skin was

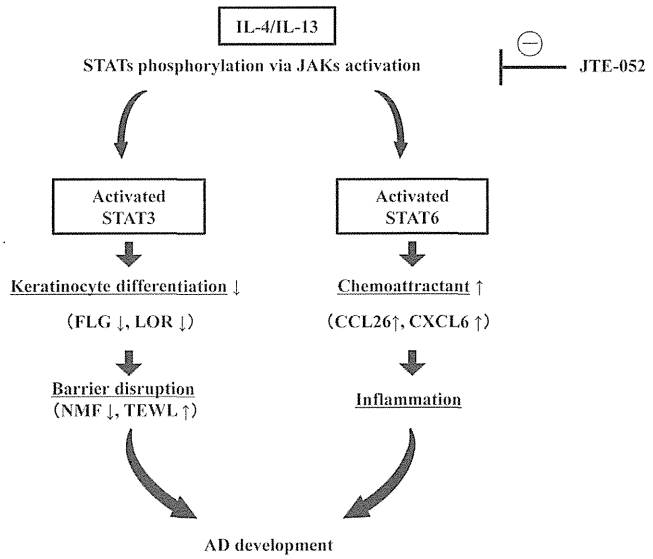

FIG 7. Model of the molecular mechanism of STATs in AD skin. IL-4 and IL-13 induce phosphorylation of STAT3 and STAT6 through JAK activation in the epidermis of patients with AD. Activated STAT3 downregulates keratinocyte differentiation–related proteins, leading to barrier disruption in accordance with decreased NMF levels and increased TEWL. On the other hand, activated STAT6 upregulates chemoattractants, such as CCL26 and CXCL6, leading to skin inflammation. Topical administration of JTE-052 inhibits phosphorylation of both STAT3 and STAT6 and normalizes barrier disruption and skin inflammation.

increased in vehicle-treated conventional mice but significantly decreased by topical application of the JAK inhibitor (Fig 4, *C*). We then measured FLG protein levels in the epidermal layers of mouse ears on day 28. In accordance with our *in vitro* findings (Fig 2, *C*), topical application of the JAK inhibitor significantly increased FLG monomer protein production compared with vehicle treatment (Fig 4, *D*, upper panel). We also found that levels of phosphorylated STAT3 and STAT6 in the epidermis in these mice were downregulated *in vivo* by JAK inhibitor treatment (Fig 4, *D*, lower panels).

In addition, we measured NMF levels in the SC of NC/Nga mice on day 28 by means of Raman microspectroscopy. NMFs are hygroscopic amino acids derived from FLG and essential for SC hydration.[39] We found that conventional mouse ears contained lower levels of NMFs than SPF mouse ears, but the JAK inhibitor treatment almost completely restored NMF levels in conventional ears to those in SPF ears (Fig 4, *E*). These findings indicate that the JAK inhibitor promotes keratinocyte differentiation and improves skin barrier function in a murine AD model.

JAK inhibitor increased NMF levels and improved barrier function in a murine dry skin model

To exclude the possibility that the JAK inhibitor's ameliorating effect on barrier dysfunction resulted only from its inhibition of immune cell activities *in vivo*, we sought to assess the effect of the JAK inhibitor on barrier function without interference from skin inflammation. To this end, we used an AEW-induced dry skin model that does not induce immune cell infiltration.[27] This dry skin model allows us to evaluate the effect of the JAK inhibitor on skin barrier function without the influence of an immune reaction. As reported previously,[27] AEW treatment (twice per day) increased TEWL in mouse ears, driving it to its peak level on day 3. Topical application of 0.5% JTE-052 (20 μL/d), on the other hand, significantly reduced TEWL (Fig 5, *A*). Quantitative PCR and immunohistochemical analysis revealed that *Flg* mRNA production and FLG and LOR protein production were enhanced by JAK inhibitor treatment compared with vehicle treatment on days 3 and 7, respectively (Fig 5, *B* and *C*). Moreover, NMFs, which had been eliminated by the AEW treatment, had recovered to a great degree on day 7 after the start of JAK inhibitor treatment (Fig 5, *D*). These data indicate that the JAK inhibitor promotes production of FLG and its cleavage product, NMF, and improves skin barrier function in a murine dry skin model.

JAK inhibitor increased FLG and NMF production in an experimental human skin graft model

Next, to address the effect of the JAK inhibitor on human skin, we prepared immunocompromised mice grafted with human skin. Vehicle and 0.5% JAK inhibitor were topically applied onto 2 different areas of each human skin graft once a day for 7 days; the 2 treatment areas were separated with petroleum jelly (Fig 6, *A*). We measured NMF levels in each area using Raman microspectroscopy and found that the total amount of NMF integrated from a depth of 0 to 28 μm of SC was significantly higher in JAK inhibitor–treated areas than in vehicle-treated areas (Fig 6, *B*). We then performed hematoxylin and eosin (H&E) staining and immunostaining of FLG in grafted skin. H&E staining identified no remarkable differences between vehicle- and JAK inhibitor–treated areas (Fig 6, *C*, upper panel), whereas FLG protein production was higher in JAK inhibitor–treated areas than in vehicle-treated areas (Fig 6, *C*, lower panel). These data indicate that the JAK inhibitor promoted terminal differentiation, even in grafted human skin.

DISCUSSION

In the present study we evaluated the role of JAK-STAT signaling in skin barrier function from the perspective of AD. Microarray analysis with a human skin equivalent model revealed that IL-4/IL-13 dominantly affected keratinocyte differentiation, presumably through JAK-STAT signaling. We also found that the JAK inhibitor JTE-052 promoted FLG and LOR protein production and that STAT3 is the key transcriptional factor in keratinocyte differentiation. Topical administration of the JAK inhibitor improved skin barrier function in accordance with increased FLG and NMF production in murine models of AD and dry skin. Consistently, the JAK inhibitor promoted NMF and FLG production in human skin tissue. These findings suggest that JAK-STAT3 signaling plays a key role in modulating keratinocyte differentiation and that the new JAK inhibitor JTE-052 has a therapeutic potential to improve skin barrier function in patients with AD.

FLG-related barrier disruption can be a primary cause of AD.[4,15,40] Consistently, we demonstrated that a compound that induces FLG expression attenuates the development of murine AD-like skin lesions.[26] However, it remains unclear how the T_H2 milieu suppresses FLG expression. Our present study using GO analysis showed that IL-4/IL-13 predominantly downregulated keratinocyte differentiation–related gene expression rather than activating immune responses. The genes that were restored

by the JAK inhibitor in the presence of IL-4/IL-13 included both *FLG* and other keratinocyte differentiation–related genes, such as *LOR*, *FLG2*, hornerin, and involucrin (Fig 1, *A*). These findings indicate that the IL-4/IL-13–JAK–STAT pathway regulates terminal keratinocyte differentiation, which is involved in skin barrier formation.[41] In addition to the terminal differentiation proteins, JTE-052 enhanced the production of NMFs in murine models of AD and dry skin and in human skin. It has recently been reported that the daily application of moisturizer reduces the risk of AD/eczema in infants.[42,43] These findings suggest that JTE-052 can reduce the risk of AD by increasing NMF production.

JAK-STATs are key transcriptional mediators that are essential for various cell functions; they are activated by several series of cytokines. Using siRNA of STATs, we demonstrated that activated STAT3 and STAT6 are involved in keratinocyte differentiation and chemokine production, respectively (Fig 7). In our results small interfering RNA for STAT3 significantly upregulated *STAT6* mRNA expression (Fig 3, *B*), indicating the possibility that STAT3 indirectly participates in the transcriptional activity of STAT6 in NHEKs. Further experiments are needed to clarify the relationship between STAT3 and STAT6 in keratinocytes. On the other hand, small interfering RNA for *STAT6* did not exhibit any effects on keratinocyte differentiation in the presence or absence of IL-4/IL-13. These data support our conclusion that STAT3 is a responsible transcriptional factor that regulates keratinocyte differentiation. It is well established that IL-4/IL-13 induces STAT6 phosphorylation,[34] which is necessary for differentiation from naive T cells to T_H2 cells.[44,45] It has been reported that STAT6 transgenic mice have spontaneous allergic dermatitis with low LOR expression levels, implying the involvement of STAT6 in the downregulation of keratinocyte differentiation.[18,46] This finding is inconsistent with our finding that STAT3, but not STAT6, is involved in keratinocyte differentiation. Of note, STAT6 transgenic mice showed high IL-4/IL-13 expression,[46] raising the possibility that the T_H2 milieu induced by STAT6 overexpression activated STAT3, which caused the LOR defect seen in these mice. Taken together, the JAK inhibitor has the potential to promote keratinocyte differentiation and inhibit immune responses in AD development. It has been reported that the pan-JAK inhibitor pyridone 6 ameliorates allergic skin inflammation of NC/Nga mice by modulating the balance of T_H2 and T_H17.[47] Our results further implicate the potential of JAK inhibitors to improve skin barrier function directly.

By using an AEW-induced dry skin model, the JAK inhibitor reduced TEWL and increased FLG mRNA/protein and NMF production. At present, the clinical significance of the above changes caused by the JAK inhibitor remains unclear. However, our findings raise the possibility that JAK/STAT inhibition might be beneficial for dry skin diseases, including asteatotic eczema. On the other hand, the skin is considered an active immune system organ that can influence systemic immunity.[48] Patients with AD often have other allergic diseases, including food allergies, asthma, and allergic rhinitis.[49] These often begin early in life and progress in a typical fashion, which is called the allergic (or atopic) march.[50] Regulating cutaneous sensitization by improving skin barrier function through regulating JAK-STAT signaling might be a possible approach to prevent the development of other allergic diseases. The next question is whether the JAK inhibitor is clinically applicable to human inflammatory skin diseases. In this study we prepared immunocompromised mice grafted with human skin to obtain human relevance and have obtained reproducible findings. It is expected that future clinical trials will reveal whether this approach is feasible to regulate AD by improving both skin inflammation and deregulated skin barrier function.

Clinical implications: Topical application of the JAK inhibitor JTE-052 has therapeutic potential to improve skin barrier function in patients with AD.

REFERENCES

1. Harding CR. The stratum corneum: structure and function in health and disease. Dermatol Ther 2004;17(suppl 1):6-15.
2. Candi E, Schmidt R, Melino G. The cornified envelope: a model of cell death in the skin. Nat Rev Mol Cell Biol 2005;6:328-40.
3. Kabashima K. New concept of the pathogenesis of atopic dermatitis: interplay among the barrier, allergy, and pruritus as a trinity. J Dermatol Sci 2013;70:3-11.
4. Palmer CN, Irvine AD, Terron-Kwiatkowski A, Zhao Y, Liao H, Lee SP, et al. Common loss-of-function variants of the epidermal barrier protein filaggrin are a major predisposing factor for atopic dermatitis. Nat Genet 2006;38:441-6.
5. McAleer MA, Irvine AD. The multifunctional role of filaggrin in allergic skin disease. J Allergy Clin Immunol 2013;131:280-91.
6. Gareus R, Huth M, Breiden B, Nenci A, Rosch N, Haase I, et al. Normal epidermal differentiation but impaired skin-barrier formation upon keratinocyte-restricted IKK1 ablation. Nat Cell Biol 2007;9:461-9.
7. Koch PJ, de Viragh PA, Scharer E, Bundman D, Longley MA, Bickenbach J, et al. Lessons from loricrin-deficient mice: compensatory mechanisms maintaining skin barrier function in the absence of a major cornified envelope protein. J Cell Biol 2000;151:389-400.
8. Kawasaki H, Nagao K, Kubo A, Hata T, Shimizu A, Mizuno H, et al. Altered stratum corneum barrier and enhanced percutaneous immune responses in filaggrin-null mice. J Allergy Clin Immunol 2012;129:1538-46.e6.
9. McGrath JA, Uitto J. The filaggrin story: novel insights into skin-barrier function and disease. Trends Mol Med 2008;14:20-7.
10. Moniaga CS, Kabashima K. Filaggrin in atopic dermatitis: flaky tail mice as a novel model for developing drug targets in atopic dermatitis. Inflamm Allergy Drug Targets 2011;10:477-85.
11. Kalinin AE, Kajava AV, Steinert PM. Epithelial barrier function: assembly and structural features of the cornified cell envelope. Bioessays 2002;24:789-800.
12. Rawlings AV, Harding CR. Moisturization and skin barrier function. Dermatol Ther 2004;17(suppl 1):43-8.
13. Thyssen JP, Kezic S. Causes of epidermal filaggrin reduction and their role in the pathogenesis of atopic dermatitis. J Allergy Clin Immunol 2014;134:792-9.
14. van den Oord RA, Sheikh A. Filaggrin gene defects and risk of developing allergic sensitisation and allergic disorders: systematic review and meta-analysis. BMJ 2009;339:b2433.
15. Gao PS, Rafaels NM, Hand T, Murray T, Boguniewicz M, Hata T, et al. Filaggrin mutations that confer risk of atopic dermatitis confer greater risk for eczema herpeticum. J Allergy Clin Immunol 2009;124:507-13, e1-7.
16. Brough HA, Simpson A, Makinson K, Hankinson J, Brown S, Douiri A, et al. Peanut allergy: Effect of environmental peanut exposure in children with filaggrin loss-of-function mutations. J Allergy Clin Immunol 2014;134:867-75.e1.
17. Howell MD, Kim BE, Gao P, Grant AV, Boguniewicz M, Debenedetto A, et al. Cytokine modulation of atopic dermatitis filaggrin skin expression. J Allergy Clin Immunol 2007;120:150-5.
18. Kim BE, Leung DY, Boguniewicz M, Howell MD. Loricrin and involucrin expression is down-regulated by Th2 cytokines through STAT-6. Clin Immunol 2008;126:332-7.
19. Guttman-Yassky E, Nograles KE, Krueger JG. Contrasting pathogenesis of atopic dermatitis and psoriasis—part I: clinical and pathologic concepts. J Allergy Clin Immunol 2011;127:1110-8.
20. Leung DY, Guttman-Yassky E. Deciphering the complexities of atopic dermatitis: shifting paradigms in treatment approaches. J Allergy Clin Immunol 2014;134:769-79.
21. Gittler JK, Krueger JG, Guttman-Yassky E. Atopic dermatitis results in intrinsic barrier and immune abnormalities: implications for contact dermatitis. J Allergy Clin Immunol 2013;131:300-13.
22. Vainchenker W, Dusa A, Constantinescu SN. JAKs in pathology: role of Janus kinases in hematopoietic malignancies and immunodeficiencies. Semin Cell Dev Biol 2008;19:385-93.

23. O'Shea JJ, Plenge R. JAK and STAT signaling molecules in immunoregulation and immune-mediated disease. Immunity 2012;36:542-50.
24. Fukushi S, Yamasaki K, Aiba S. Nuclear localization of activated STAT6 and STAT3 in epidermis of prurigo nodularis. Br J Dermatol 2011;165:990-6.
25. Tanimoto A, Ogawa Y, Oki C, Kimoto Y, Nozawa K, Amano W, et al. Pharmacological properties of JTE-052: a novel potent JAK inhibitor that suppresses various inflammatory responses in vitro and in vivo. Inflamm Res 2015;64:41-51.
26. Otsuka A, Doi H, Egawa G, Maekawa A, Fujita T, Nakamizo S, et al. Possible new therapeutic strategy to regulate atopic dermatitis through upregulating filaggrin expression. J Allergy Clin Immunol 2014;133:139-46, e1-10.
27. Miyamoto T, Nojima H, Shinkado T, Nakahashi T, Kuraishi Y. Itch-associated response induced by experimental dry skin in mice. Jpn J Pharmacol 2002;88:285-92.
28. Kupershmidt I, Su QJ, Grewal A, Sundaresh S, Halperin I, Flynn J, et al. Ontology-based meta-analysis of global collections of high-throughput public data. PLoS One 2010;5:e13066.
29. Nomura I, Goleva E, Howell MD, Hamid QA, Ong PY, Hall CF, et al. Cytokine milieu of atopic dermatitis, as compared to psoriasis, skin prevents induction of innate immune response genes. J Immunol 2003;171:3262-9.
30. Ashburner M, Ball CA, Blake JA, Botstein D, Butler H, Cherry JM, et al. Gene ontology: tool for the unification of biology. The Gene Ontology Consortium. Nat Genet 2000;25:25-9.
31. Guttman-Yassky E, Suarez-Farinas M, Chiricozzi A, Nograles KE, Shemer A, Fuentes-Duculan J, et al. Broad defects in epidermal cornification in atopic dermatitis identified through genomic analysis. J Allergy Clin Immunol 2009; 124:1235-44.e58.
32. Sandilands A, Sutherland C, Irvine AD, McLean WH. Filaggrin in the frontline: role in skin barrier function and disease. J Cell Sci 2009;122:1285-94.
33. Madden KB, Whitman L, Sullivan C, Gause WC, Urban JF Jr, Katona IM, et al. Role of STAT6 and mast cells in IL-4- and IL-13-induced alterations in murine intestinal epithelial cell function. J Immunol 2002;169:4417-22.
34. Umeshita-Suyama R, Sugimoto R, Akaiwa M, Arima K, Yu B, Wada M, et al. Characterization of IL-4 and IL-13 signals dependent on the human IL-13 receptor alpha chain 1: redundancy of requirement of tyrosine residue for STAT3 activation. Int Immunol 2000;12:1499-509.
35. Owczarek W, Paplinska M, Targowski T, Jahnz-Rozyk K, Paluchowska E, Kucharczyk A, et al. Analysis of eotaxin 1/CCL11, eotaxin 2/CCL24 and eotaxin 3/CCL26 expression in lesional and non-lesional skin of patients with atopic dermatitis. Cytokine 2010;50:181-5.
36. Kagami S, Saeki H, Komine M, Kakinuma T, Tsunemi Y, Nakamura K, et al. Interleukin-4 and interleukin-13 enhance CCL26 production in a human keratinocyte cell line, HaCaT cells. Clin Exp Immunol 2005;141:459-66.
37. Suto H, Matsuda H, Mitsuishi K, Hira K, Uchida T, Unno T, et al. NC/Nga mice: a mouse model for atopic dermatitis. Int Arch Allergy Immunol 1999; 120(suppl 1):70-5.
38. Proksch E, Folster-Holst R, Jensen JM. Skin barrier function, epidermal proliferation and differentiation in eczema. J Dermatol Sci 2006;43:159-69.
39. Kezic S, Kemperman PM, Koster ES, de Jongh CM, Thio HB, Campbell LE, et al. Loss-of-function mutations in the filaggrin gene lead to reduced level of natural moisturizing factor in the stratum corneum. J Invest Dermatol 2008; 128:2117-9.
40. Elias PM, Schmuth M. Abnormal skin barrier in the etiopathogenesis of atopic dermatitis. Curr Opin Allergy Clin Immunol 2009;9:437-46.
41. Hardman MJ, Sisi P, Banbury DN, Byrne C. Patterned acquisition of skin barrier function during development. Development 1998;125:1541-52.
42. Horimukai K, Morita K, Narita M, Kondo M, Kitazawa H, Nozaki M, et al. Application of moisturizer to neonates prevents development of atopic dermatitis. J Allergy Clin Immunol 2014;134:824-30.e6.
43. Simpson EL, Chalmers JR, Hanifin JM, Thomas KS, Cork MJ, McLean WH, et al. Emollient enhancement of the skin barrier from birth offers effective atopic dermatitis prevention. J Allergy Clin Immunol 2014;134:818-23.
44. Ashino S, Takeda K, Li H, Taylor V, Joetham A, Pine PR, et al. Janus kinase 1/3 signaling pathways are key initiators of TH2 differentiation and lung allergic responses. J Allergy Clin Immunol 2014;133:1162-74.
45. Kaplan MH, Schindler U, Smiley ST, Grusby MJ. Stat6 is required for mediating responses to IL-4 and for development of Th2 cells. Immunity 1996; 4:313-9.
46. Sehra S, Yao Y, Howell MD, Nguyen ET, Kansas GS, Leung DY, et al. IL-4 regulates skin homeostasis and the predisposition toward allergic skin inflammation. J Immunol 2010;184:3186-90.
47. Nakagawa R, Yoshida H, Asakawa M, Tamiya T, Inoue N, Morita R, et al. Pyridone 6, a pan-JAK inhibitor, ameliorates allergic skin inflammation of NC/Nga mice via suppression of Th2 and enhancement of Th17. J Immunol 2011;187:4611-20.
48. Egawa G, Kabashima K. Skin as a peripheral lymphoid organ: revisiting the concept of skin-associated lymphoid tissues. J Invest Dermatol 2011;131: 2178-85.
49. Akdis CA, Akdis M, Bieber T, Bindslev-Jensen C, Boguniewicz M, Eigenmann P, et al. Diagnosis and treatment of atopic dermatitis in children and adults: European Academy of Allergology and Clinical Immunology/American Academy of Allergy, Asthma and Immunology/PRACTALL Consensus Report. Allergy 2006;61:969-87.
50. Heimall J, Spergel JM. Filaggrin mutations and atopy: consequences for future therapeutics. Expert Rev Clin Immunol 2012;8:189-97.

METHODS

Microarray

Cy3-labeled complementary RNA was synthesized from RNA by using a Low Input Quick Amp Labeling Kit (Agilent Technologies, Santa Clara, Calif). Six hundred nanograms of complementary RNAs were fragmented and hybridized for 17 hours at 65°C to Agilent SurePrint G3 Human Gene Expression Microarray 8 × 60 K (#G4851A, Agilent Technologies). The microarray slides were scanned with the Agilent DNA Microarray Scanner System (#G2565AA, Agilent Technologies) and analyzed with Feature Extraction Software (version 11.0.1.1, Agilent Technologies). Microarray data were analyzed in GeneSpring GX (version 12.6, Agilent Technologies). Signal values of each probe were normalized to the 75th percentile of all samples and the mean value for the probe of vehicle-treated samples. Genes with different expressions were extracted by using a moderated *t* test and subjected to the Benjamini and Hochberg method for correction of *P* values for multiple testing (corrected $P < .05$) and 2-fold change. Hierarchic clustering was performed in genes differentially expressed on IL-4/IL-13–treated samples by using Euclidean distance and the Ward linkage rule. NextBio software (www.nextbio.com) was used for GO analysis and for the comparison of the obtained data set (Bioset [Bs]) described above with the publicly available data set.[E1] The difference in numbers between the common Venn diagram (Fig 1, *C* and *D*) and bar graph (Fig E1, *A-C*) is derived from duplication of the probes for some genes.

Quantitative RT-PCR analysis

Quantitative RT-PCR analysis was performed, as described previously.[E2] All primers were obtained from Greiner Japan (Tokyo, Japan). The primer sequences were as follows: *FLG*, 5′-TCG GCA AAT CCT GAA GAA TCC AGA-3′ (forward) and 5′-GCT TGA GCC AAC TTG AAT AAT ACC ATC AG′ (reverse); *LOR*, 5′-CTC TGT CTG CGG CTA CTC TG-3′ (forward) and 5′-CAC GAG GTC TGA GTG ACC TG-3′ (reverse); human *STAT3*, 5′-GGC GTC ACT TTC ACT TGG GT-3′ (forward) and 5′-CCA CGG ACT GGA TCT GGG T-3′ (reverse); *STAT6*, 5′-GCC AAA GCC CTA GTG CTG AA-3′ (forward) and 5′-GAC GAG GGT TCT CAG GAC TTC-3′ (reverse); and *CCL26*, 5′-AAC TCC GAA ACA ATT GTG ACT CAG CTG′ (forward) and 5′-GTA ACT CTG GGA GGA AAC ACC CTC TCC-3′ (reverse). Results were normalized to those of the housekeeping gene glyceraldehyde-3-phosphate dehydrogenase *(GAPDH)*, according to the method based on change in the Δ cycle threshold (ΔC_T) and calculated based on $2^{-\Delta CT}$.

Immunoblotting

Proteins were obtained from cells and tissues, as described previously.[E3] The samples were used for immunoblotting with either 1:500 dilution of anti-FLG antibody (Santa Cruz Biotechnology, Dallas, Tex), 1:1,000 dilution of anti-LOR antibody (Covance, Berkeley, Calif), 1:2,000 dilution of STAT3 and anti-phosphorylated STAT3 antibody (Cell Signaling Technology, Beverly, Mass), 1:1,000 dilution of anti-STAT6 and anti-phosphorylated STAT6 antibody (Cell Signaling Technology), or 1:10,000 dilution of anti–glyceraldehyde-3-phosphate dehydrogenase antibody (Sigma-Aldrich, St Louis, Mo), followed by horseradish peroxidase–conjugated anti-mouse or anti-rabbit IgG (GE Healthcare, Waukesha, Wis). The blotting was then developed by means of chemiluminescence (GE Healthcare).

Histology and immunostaining

Cells were fixed with 4% paraformaldehyde and then permeabilized with methanol before staining. Cells were probed with anti–β-actin antibody (Sigma-Aldrich) and anti-STAT3 or anti-STAT6 antibody (Cell Signaling Technology) and then incubated with Alexa Fluor 546–coupled (for β-actin) and Alexa Fluor 488–coupled (for STATs) secondary antibodies (Life Technologies, Carlsbad, Calif).

Tissues were fixed with 4% paraformaldehyde in PBS and then embedded in paraffin. Sections with a thickness of 5 μm were deparaffinized and stained with H&E. For immunostaining, sections with a thickness of 5 μm were deparaffinized, and antigens were retrieved by using Cell Conditioning 1 (Roche, Basel, Switzerland), incubated with 1:300 dilution of anti-filaggrin antibody (Santa Cruz Biotechnology) or 1:1000 dilution of anti-loricrin antibody (Covance, Princeton, NJ), and then incubated with Alexa Fluor 488–coupled secondary antibody. The slides were mounted in ProLong Gold Antifade reagent (Invitrogen). All images were obtained with a BIOREVO BZ-9000 system (Keyence, Osaka, Japan).

Evaluation of skin conditions

The clinical severity of NC/Nga mice was scored according to the macroscopic diagnostic criteria for these genotype.[E4] In brief, the total clinical score for skin lesions was designated as the sum of individual scores of the right ear, left ear, dorsum, and face, each graded as 0 (none), 1 (mild), or 2 (severe) for the symptoms of erythema/hemorrhage, edema, crust, excoriation/erosion, and scaling/dryness. Clinical scores were evaluated once every week.

TEWL of the surface of the skin was measured at room temperature (23°C-26°C) at 40% to 60% humidity with a VAPOSCAN AS-VT100RS machine (Asahi Biomed, Yokohama, Japan). The individual value for each mouse was calculated as the median of 2 consecutive measurements.

Murine and human NMF profiles were measured by using *in vivo* confocal Raman microspectroscopy (River Diagnostics, Rotterdam, The Netherlands) at intervals of 1 μm to a depth of 8 μm and those of grafted human skin at intervals of 4 μm to a depth of 28 μm. Results were analyzed with the SkinTools 2.0 software package (River Diagnostics). Each NMF concentration in the SC of murine or human skin was calculated as the median of 5 or 10 consecutive measurements, respectively.

Antigen-induced chronic allergic dermatitis model

Antigen-induced chronic allergic dermatitis was induced, as previously described.[E5] Briefly, NC/Nga mice were intradermally injected at the ventral side of their ear with 5 μg of mite allergen extract (Cosmo Bio LSL, Tokyo, Japan) in saline on days 0, 2, 4, 7, 9, 11, 14, and 16. Ear thickness was measured 24 hours after each injection of antigen with a digital thickness gauge (Mitsutoyo, Kanagawa, Japan). For oral administration of drugs, JTE-052 or cyclosporine (Wako, Japan) was suspended in 0.5% methylcellulose (Wako, Japan) and administered to mice once daily from days 0 to 16. For topical application of drugs, JTE-052 (1% ointment [wt/wt]) or tacrolimus (0.1% Protopic; Astellas, Tokyo, Japan) was topically applied to both sides of the ear once daily from days 0 to 16. Each drug was administered 1 hour before each injection of antigen.

REFERENCES

E1. Guttman-Yassky E, Suarez-Farinas M, Chiricozzi A, Nograles KE, Shemer A, Fuentes-Duculan J, et al. Broad defects in epidermal cornification in atopic dermatitis identified through genomic analysis. J Allergy Clin Immunol 2009; 124:1235-44.e58.

E2. Nakajima S, Honda T, Sakata D, Egawa G, Tanizaki H, Otsuka A, et al. Prostaglandin I2-IP signaling promotes Th1 differentiation in a mouse model of contact hypersensitivity. J Immunol 2010;184:5595-603.

E3. Otsuka A, Doi H, Egawa G, Maekawa A, Fujita T, Nakamizo S, et al. Possible new therapeutic strategy to regulate atopic dermatitis through upregulating filaggrin expression. J Allergy Clin Immunol 2014;133:139-46, e1-10.

E4. Suto H, Matsuda H, Mitsuishi K, Hira K, Uchida T, Unno T, et al. NC/Nga mice: a mouse model for atopic dermatitis. Int Arch Allergy Immunol 1999; 120(suppl 1):70-5.

E5. Hirai T, Yoshikawa T, Nabeshi H, Yoshida T, Tochigi S, Ichihashi K, et al. Amorphous silica nanoparticles size-dependently aggravate atopic dermatitis-like skin lesions following an intradermal injection. Part Fibre Toxicol 2012;9:3.

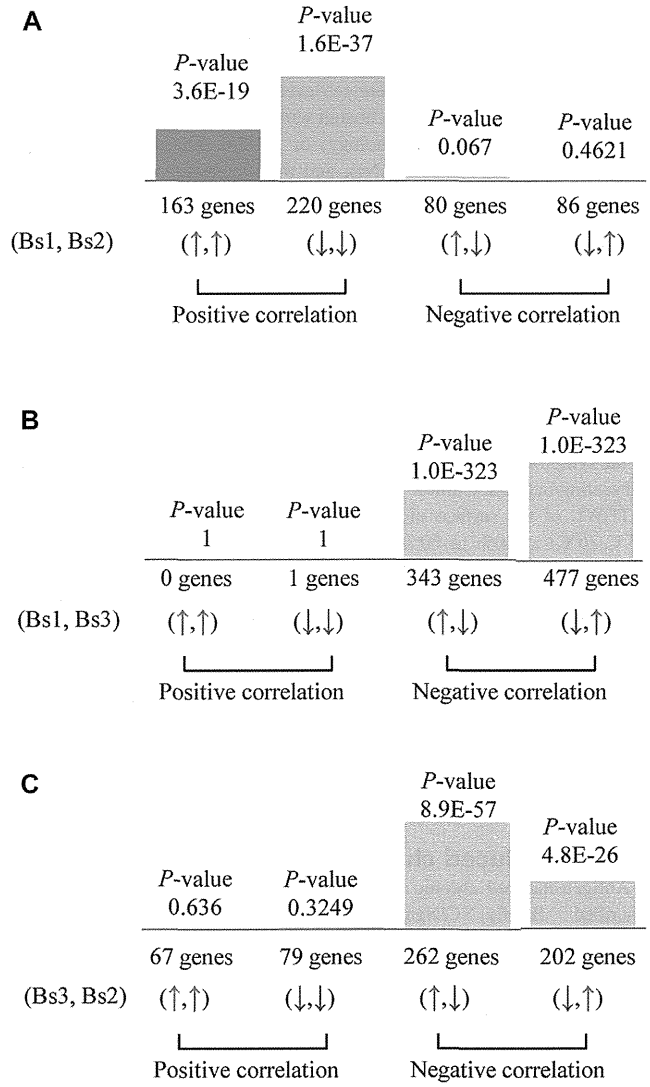

FIG E1. Correlation analyses between gene expression changes. **A,** Correlation analysis between genes differentially expressed in IL-4/IL-13–treated samples compared with vehicle-treated samples (Bioset; Bs1) and genes with altered expression in AD skin compared with healthy control skin (Bs2). **B,** Correlation analysis between the genes differentially expressed on IL-4/IL-13 plus JTE-052–treated samples compared with IL-4/IL-13–treated samples (Bs3) and Bs1. **C,** Correlation analysis between Bs2 and Bs3. The *bars* indicate *P* values of each correlation. *Arrows* indicate the direction of gene expression (*red*, upregulation; *blue*, downregulation).

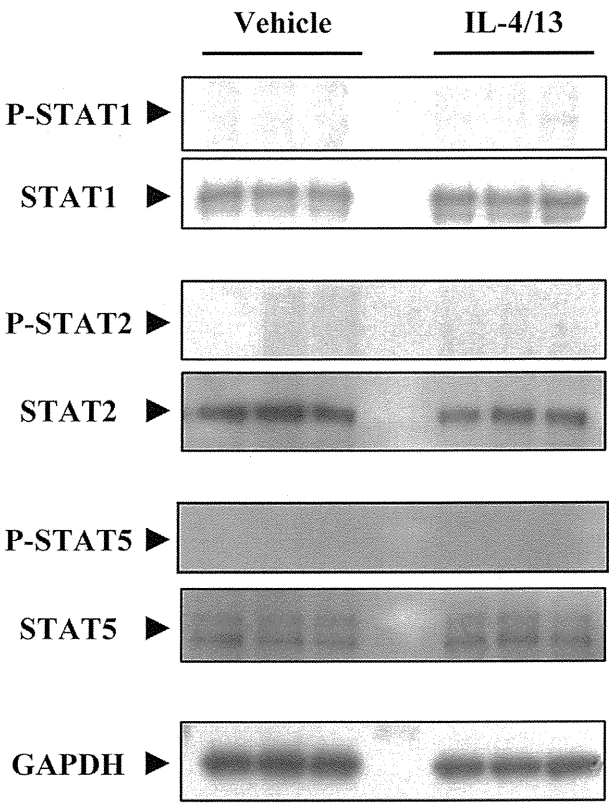

FIG E2. Phosphorylation of STAT1, STAT2, and STAT5 in the presence or absence of IL-4/IL-13 in TESTSKIN by using Western blotting.

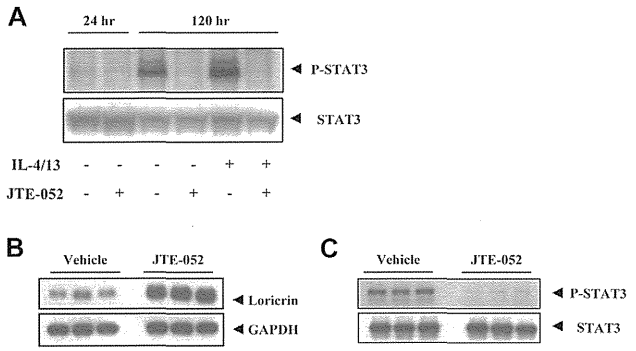

FIG E3. Phosphorylation of STAT3 in NHEKs. **A,** NHEKs were incubated in the presence or absence of 100 ng/mL IL-4/IL-13 with or without 1000 nmol/L JTE-052 for 24 or 120 hours. **B** and **C**, Effects of JTE-052 on phosphorylation of STAT3 (Fig E3, *B*) and LOR protein production (Fig E3, *C*) in TESTSKIN.

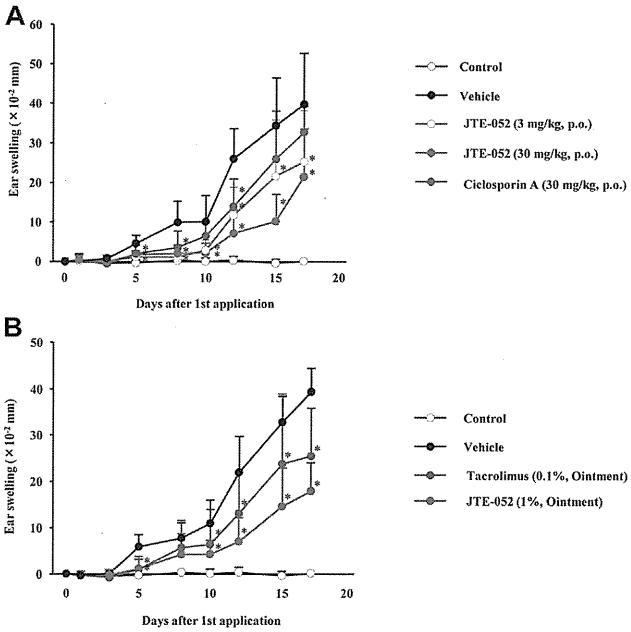

FIG E4. The JAK inhibitor ameliorated ear-swelling responses in an antigen-induced chronic allergic dermatitis model in NC/Nga mice. Mice were orally administrated with JTE-052 or cyclosporine **(A)** or topically applied with JTE-052 or tacrolimus **(B)** once daily. $*P < .05$ versus vehicle (Dunnett or Steel test).

TABLE E1. List of the 100 genes most strongly upregulated in TESTSKIN by means of treatment with IL-4/IL-13

Rank	Fold change	Gene symbol	Gene name
1	941.4	*TNFAIP6*	TNF, alpha-induced protein 6
2	459.7	*CCL26*	Chemokine (C-C motif) ligand 26
3	336.3	*CAPN14*	Calpain 14
4	182.2	*IGFL4*	IGF-like family member 4
5	131.9	*CLDN5*	Claudin 5
6	116.2	*NTRK1*	Neurotrophic tyrosine kinase, receptor, type 1
7	105.2	*EMILIN2*	Elastin microfibril interfacer 2
8	91.5	*CH25H*	Cholesterol 25-hydroxylase
9	85.3	*TREML2*	Triggering receptor expressed on myeloid cells-like 2
10	71.4	*HSD3B1*	Hydroxy-delta-5-steroid dehydrogenase, 3 beta- and steroid delta-isomerase 1
11	71.3	*CHGA*	Chromogranin A (parathyroid secretory protein 1)
12	54.3	*KALRN*	Kalirin, RhoGEF kinase
13	49.3	*PMP22*	Peripheral myelin protein 22
14	42.5	*SLC16A14*	Solute carrier family 16, member 14
15	41.5	*CXCL6*	Chemokine (C-X-C motif) ligand 6
16	40.2	*MAOB*	Monoamine oxidase B
17	36.9	*CCL2*	Chemokine (C-C motif) ligand 2
18	33.5	*PIP*	Prolactin-induced protein
19	33.1	*GKN1*	Gastrokine 1
20	25.5	*GLDC*	Glycine dehydrogenase (decarboxylating)
21	23.5	*LOXL4*	Lysyl oxidase-like 4
22	22.6	*DPP4*	Dipeptidyl-peptidase 4
23	21.2	*CDC45*	Cell division cycle 45
24	21.0	*TNC*	Tenascin C
25	20.5	*ANO1*	Anoctamin 1, calcium activated chloride channel
26	19.4	*NFE2*	Nuclear factor, erythroid 2
27	19.4	*IL13RA2*	IL-13 receptor, alpha 2
28	19.1	*FAM124B*	Family with sequence similarity 124B
29	18.7	*SH2D1B*	SH2 domain containing 1B
30	17.0	*FAM101A*	Family with sequence similarity 101, member A
31	15.8	*HS3ST1*	Heparan sulfate (glucosamine) 3-O-sulfotransferase 1
32	15.6	*COL4A4*	Collagen, type IV, alpha 4
33	15.6	*POLR2M*	Polymerase (RNA) II (DNA directed) polypeptide M
34	14.1	*IL10RA*	IL-10 receptor, alpha
35	13.8	*LBH*	Limb bud and heart development
36	13.6	*RASGRP1*	RAS guanyl releasing protein 1 (calcium and DAG-regulated)
37	13.2	*KAL1*	Kallmann syndrome 1 sequence
38	12.4	*C10orf82*	Chromosome 10 open reading frame 82
39	11.9	*KCNJ2*	Potassium inwardly-rectifying channel, subfamily J, member 2
40	11.8	*OXTR*	Oxytocin receptor
41	11.8	*SOCS1*	Suppressor of cytokine signaling 1
42	11.5	*TNFSF13*	TNF (ligand) superfamily, member 13
43	11.4	*SPP1*	Secreted phosphoprotein 1
44	11.2	*C15orf27*	Chromosome 15 open reading frame 27
45	11.0	*BMP4*	Bone morphogenetic protein 4
46	10.8	*NID2*	Nidogen 2 (osteonidogen)
47	10.6	*CFI*	Complement factor I
48	10.5	*NES*	Nestin
49	10.3	*CISH*	Cytokine inducible SH2-containing protein
50	10.3	*LOC388780*	Uncharacterized LOC388780
51	10.0	*CFB*	Complement factor B
52	9.8	*MME*	Membrane metalloendopeptidase
53	9.7	*IL8*	IL-8
54	9.6	*KCNJ12*	Potassium inwardly-rectifying channel, subfamily J, member 12
55	9.6	*LY75*	Lymphocyte antigen 75
56	9.2	*MATK*	Megakaryocyte-associated tyrosine kinase
57	9.0	*SLC26A2*	Solute carrier family 26 (anion exchanger), member 2
58	9.0	*TTYH2*	Tweety family member 2
59	8.9	*DUOX2*	Dual oxidase 2
60	8.8	*SALL4*	Spalt-like transcription factor 4
61	8.7	*PRSS53*	Protease, serine, 53
62	8.6	*PRR9*	Proline rich 9

(Continued)

TABLE E1. *(Continued)*

Rank	Fold change	Gene symbol	Gene name
63	8.5	*ABCC2*	ATP-binding cassette, sub-family C (CFTR/MRP), member 2
64	8.3	*C1QTNF1-AS1*	C1QTNF1 antisense RNA 1
65	8.2	*SLC7A4*	Solute carrier family 7, member 4
66	8.1	*SUSD2*	Sushi domain containing 2
67	7.7	*SEMA3E*	Sema domain, immunoglobulin domain (Ig), short basic domain, secreted, (semaphorin) 3E
68	7.5	*FZD10*	Frizzled family receptor 10
69	7.4	*MB*	Myoglobin
70	7.3	*CAMP*	Cathelicidin antimicrobial peptide
71	7.2	*RGS4*	Regulator of G-protein signaling 4
72	7.1	*EML5*	Echinoderm microtubule associated protein like 5
73	7.1	*SIDT1*	SID1 transmembrane family, member 1
74	6.9	*DAPK2*	Death-associated protein kinase 2
75	6.8	*CXCL1*	Chemokine (C-X-C motif) ligand 1 (melanoma growth stimulating activity, alpha)
76	6.7	*PPP1R3C*	Protein phosphatase 1, regulatory subunit 3C
77	6.7	*TMEM71*	Transmembrane protein 71
78	6.6	*ANPEP*	Alanyl (membrane) aminopeptidase
79	6.6	*FGF19*	Fibroblast growth factor 19
80	6.6	*MMP12*	Matrix metallopeptidase 12 (macrophage elastase)
81	6.5	*AFP*	Alpha-fetoprotein
82	6.4	*CD200R1*	CD200 receptor 1
83	6.3	*OSBPL1A*	Oxysterol binding protein-like 1A
84	6.3	*TPK1*	Thiamin pyrophosphokinase 1
85	6.2	*NEK10*	NIMA-related kinase 10
86	6.2	*RASL11B*	RAS-like, family 11, member B
87	6.1	*PDE9A*	Phosphodiesterase 9A
88	6.1	*SLCO2A1*	Solute carrier organic anion transporter family, member 2A1
89	6.1	*PLSCR4*	Phospholipid scramblase 4
90	6.0	*CIITA*	Class II, major histocompatibility complex, transactivator
91	6.0	*CXCL11*	Chemokine (C-X-C motif) ligand 11
92	6.0	*RTP4*	Receptor (chemosensory) transporter protein 4
93	6.0	*LURAP1L*	Leucine rich adaptor protein 1-like
94	5.9	*COL6A2*	Collagen, type VI, alpha 2
95	5.9	*CXCL2*	Chemokine (C-X-C motif) ligand 2
96	5.6	*APOBEC3A*	Apolipoprotein B mRNA editing enzyme, catalytic polypeptide-like 3A
97	5.6	*CSF3*	Colony-stimulating factor 3 (granulocyte)
98	5.6	*MAT1A*	Methionine adenosyltransferase I, alpha
99	5.5	*ST6GAL1*	ST6 beta-galactosamide alpha-2,6-sialyltranferase 1
100	5.4	*ZNF326*	Zinc finger protein 326

Le sommaire de ce numéro

http://www.john-libbey-eurotext.fr/fr/revues/medecine/ejd/sommaire.md?type=text.html

Montrouge, le 07-12-2015

Takaaki Hanafusa

Vous trouverez ci-après le tiré à part de votre article au format électronique (pdf) :
Possible association of anti-tumor necrosis factor-α antibody therapy with the development of scleroderma-like changes with lichen planus

paru dans
European Journal of Dermatology, 2015, Volume 25, Numéro 5

John Libbey Eurotext

Histopathological examination of the neck lesion revealed large areas of caseation necrosis surrounded by lymphocytes, neutrophils, plasma cells and Langhans-type giant cells *(figure 1D)*. The leg lesions revealed mainly lobular panniculitis accompanied by granulomatous inflammation, fat necrosis, giant cells, and vasculitis *(figures 1E-F)* but no caseation necrosis. Ziehl-Neelsen staining showed no acid-fast bacilli in either specimen. We diagnosed the patient with EIB of the legs associated with scrofuloderma of the right neck and right axilla. Treatment with isoniazid 300 mg, rifampicin 450 mg, and ethambutol 750 mg for 3 months resulted in remarkable improvement of all skin lesions.

Scrofuloderma begins as painless subcutaneous nodules caused by MTB disseminated from extracutaneous tuberculosis to the skin. The most common location of active tuberculosis causing scrofuloderma is the cervical lymph-nodes [1]. EIB is considered a multifactorial disorder with many different causes, including MTB allergy (tuberculid). Tuberculids are considered to be hypersensitivity reactions to MTB or their fragments. Koga *et al.* reported in a case of EIB with active tuberculosis of the axillary lymph-nodes, that PPD-specific T cells capable of producing IFN-γ are likely involved in the formation of EIB as a type of delayed-type hypersensitivity response to MTB antigens at the site of the skin lesions [2, 3].

The association between lymph-node tuberculosis and EIB has been previously reported. Shimizu *et al.* reported that EIB more frequently involved lymph-node tuberculosis than other active tuberculosis lesions [1]. Although reports of EIB with lymph-node tuberculosis are rare in the English medical literature, they are not uncommon in the Japanese medical literature. This is possibly due to an epidemic of MTB infection in Japan and the difficulty of diagnosing lymph-node tuberculosis. Because Japan has many patients with MTB infection and adequate diagnostic technology for tuberculosis, reports of EIB with lymph-node tuberculosis might be relatively common.

Remarkably, we could not find cases of EIB with scrofuloderma as a consequence of lymph-node tuberculosis in the English medical literature, except for the present case. This is possibly due to the fact that the quantity of MTB in the pus and tissue of the scrofuloderma is low, so that the delayed-type hypersensitivity reaction to MTB might be less likely to occur [4, 5]. It is possible that the two widespread scrofuloderma lesions in our patient may have been closely involved with the development of EIB; however, the reason why reports of EIB with scrofuloderma are rare remains unclear. ■

Disclosure. *Financial support: none. Conflict of interest: none.*

[1] Department of Dermatology, Hirosaki University Graduate School of Medicine, 5 Zaifu-cho, Hirosaki 036-8562, Japan
[2] Department of Dermatology, Aomori Prefectural Central Hospital, Aomori, Japan
<m981027@hirosaki-u.ac.jp>

Ayumi KOREKAWA[1]
Hajime NAKANO[1]
Daisuke SAWAMURA[1]
Hideo KITAMURA[2]
Ken HARADA[2]

1. Shimizu A, Takahashi A, Negishi I, *et al.* The close association of Lymphadenitis tuberculosa and Erythema induratum of Bazin in Japanese patients. *Dermatology* 2003; 207: 426-7.
2. Thomas PA, Schraut W, Korting HC, *et al.* Papulo-necrotic tuberculids and erythema induratum (of Bazin) in a patient with a history of tuberculosis: role of specific T cells. *Eur J Dermatol* 1993; 3: 97-101.
3. Koga T, Kubota Y, Kiryu H, *et al.* Erythema induratum in a patient with active tuberculosis of the axillary lymph node: IFN-gamma release of specific T cells. *Eur J Dermatol* 2001; 11: 48-9.
4. Usuki K, Kodama K, Yotsumoto S, *et al.* A case of scrofuloderma with incredible cervical lymph node tuberculosis. *Rinsho Derma (Tokyo)* 2001; 55: 511-3.
5. Yano T, Shinoda S, Daikoku H. A case of scrofuloderma. *Practical Dermatol* 1993; 55: 910.

doi:10.1684/ejd.2015.2625

Possible association of anti-tumor necrosis factor-α antibody therapy with the development of scleroderma-like changes with lichen planus

A 42-year-old Japanese woman presented with systemic skin sclerosis and erythema as well as back erosions in July 2012. She had developed intractable oral aphtha 8 years before. Depigmentation, which appeared on the neck and axilla, was resistant to narrow-band ultraviolet B therapy (nbUVB) during a previous clinic visit in 2005. Psoriasis-like lesions appeared around the patient's waist and developed on her entire body in January 2011 *(figure 1A)*. The patient was diagnosed with psoriasis vulgaris on the basis of the clinical findings without histological examination and was administered adalimumab, a fully human anti-tumor necrosis factor (TNF)-α antibody, for 2 months. However, 6 months after the anti-TNF-α antibody treatment, skin erythema, sclerosis, pigmentation and depigmentation worsened, followed by the development of skin erosions on her back and waist and a fever above 38 °C *(figure 1B)*. An intractable oral aphtha was also present *(figure 1C)*. Therefore, the patient was admitted to our hospital for an extensive examination in September 2012. The modified Rodnan total skin thickness score (MRSS) was 38. The results of the blood test, including complete blood count, renal and liver function and C-reactive protein level, were normal. IgG level was elevated at 2164 mg/dL (normal range: 870-1700), whereas IgM and IgA levels were normal. Complement component (C) 4 level was decreased at 4 mg/dL (17-45), whereas that of C3 was normal. Tests for antinuclear antibody, anti-topoisomerase I, anti-centromere, anti-RNP and anti-SS-A antibodies yielded negative results. The patient was also found to have hypothyroidism. Flow cytometric analysis revealed that $CD4^+$ $CD25^+$ $Foxp3^+$ regulatory T cells (Treg) were not decreased in the peripheral blood. The patient had never undergone bone marrow or stem cell transplantation, or blood transfusion. No thymoma was noted but systemic lymph node swelling was detected by contrast-enhanced computed tomography. The findings of a skin biopsy taken from regions of skin sclerosis and scaly erythema were scleroderma-like changes and lichen